2020 16th Specialist Meeting on Microwave Radiometry and Remote Sensing for the Environment (MicroRad) | 978-1-7281-7093-0/20/$31.00 ©2020 IEEE | DOI: 10.1109/MicroRad49612.2020.9342539

Spatio-Temporal Resolution Enhancement for Geostationary Microwave Data

Igor Yanovsky*†, Jing Qin‡ and Bjorn Lambrigtsen*
*Jet Propulsion Laboratory, California Institute of Technology, Pasadena, CA, USA
†Joint Institute for Regional Earth System Science and Engineering, University of California, Los Angeles, CA, USA
‡Department of Mathematics, University of Kentucky, Lexington, KY, USA

***Abstract*—In this paper, we provide a formulation for enhancing the spatio-temporal resolution of a remote sensing sequence of images. Such an image sequence could be captured by a sensor that convolves a physical scene with a spatio-temporal point spread function whose two-dimensional spatial component is the microwave instrument's point spread function and whose one-dimensional temporal component is the rectangular kernel with sensor exposure time as its support. We perform resolution enhancement in the space-time domain, as opposed to solving the deconvolution problem for each observation. Simultaneous space-time optimization achieves a more efficient and more accurate reconstruction. The proposed deconvolution method employs total variation regularization and solves the formulation via the Split-Bregman optimization algorithm. In our experiments, we use a simulated microwave image sequence of a hurricane and demonstrate that the proposed methodology improves the accuracy when compared to the observed sequence.**

***Index Terms*—Geostationary satellite, microwave imaging, remote sensing, spatio-temporal resolution, super-resolution**

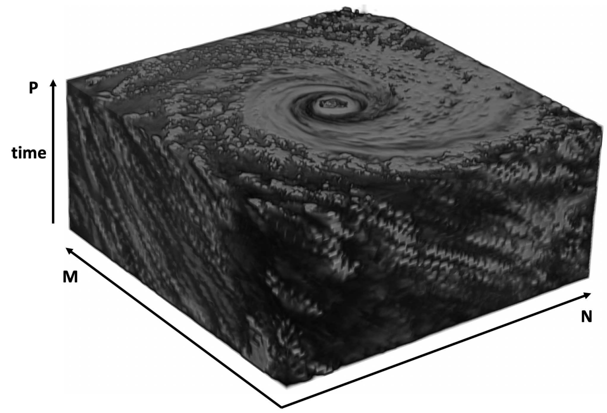

Fig. 1. Spatio-temporal sequence of P images. Each image has $M \times N$ pixels.

I. Introduction

Resolution of a microwave sensor is limited in space and in time. In particular, a microwave aperture synthesis system is known to have spatial blurring and distortion. This results in ringing near features in the observations. On the other hand, exposure time and frame-rate limit the temporal resolution of the sensor. Temporal blur can be considered as a convolution of the ground truth with a rectangular function in time. Resolution enhancement could be performed in the space-time domain, as opposed to solving the deconvolution problem for each observation. Simultaneous space-time optimization will achieve a more efficient and more accurate reconstruction.

A variety of independent spatial and temporal super-resolution methods have been proposed. Spatial resolution enhancement techniques were introduced in [1]–[9], and temporal resolution enhancement techniques were introduced in [10]–[13]. We have previously proposed methodologies to enhance spatial resolution and temporal resolution separately, but not both at the same time [14]–[16]. Specifically, we solved the super-resolution problems using total variation (TV) regularization, efficient Split-Bregman, and alternating direction method of multipliers (ADMM) techniques. In these previous works, we reconstructed images that were convolved with spatial PSF [14] or image sequences convolved by temporal averaging [16]. The deconvolution problem in the presence of noise is ill-posed. Therefore, we needed to apply regularization to guarantee the existence and uniqueness of the solution while preserving its geometric characteristics. We used the total variation (TV) regularization [17] to solve the reconstruction problem within the energy minimization formulation for each spatial and temporal resolution enhancement. TV minimizationn preserves the features in an image. We used the Split Bregman method [18] to solve the TV deconvolution problem. The Split Bregman method allows achieving fast and robust computation of the reconstruction.

There has been ongoing research in mixed spatio-temporal resolution enhancement methods. In [19], multiple low resolution video sequences were used to reconstruct a high resolution space-time video sequence. In [20], the authors proposed a fast space-time algorithm involving TV regularization and ADMM for restoring video sequences. In this work, which is based on our aforementioned previous works on spatial and temporal deconvolution, we construct a spatio-temporal resolution enhancement formulation using a variational approach. We use the Split-Bregman method and total variation minimization to

This research was carried out in part at the Jet Propulsion Laboratory, California Institute of Technology, under a contract with the National Aeronautics and Space Administration. The research of Qin is supported by the NSF grant DMS-1941197.

978-1-7281-7093-0/20/$31.00 ©2020 IEEE

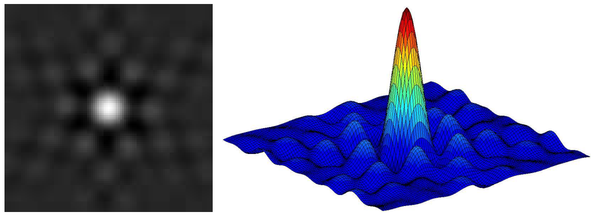

Fig. 2. Point spread function (PSF) of the GeoSTAR instrument. An aperture synthesis system is characterized by the PSF that is a 2-D sinc-like function with positive and negative sidelobes, which blurs the resulting images and creates artifacts.

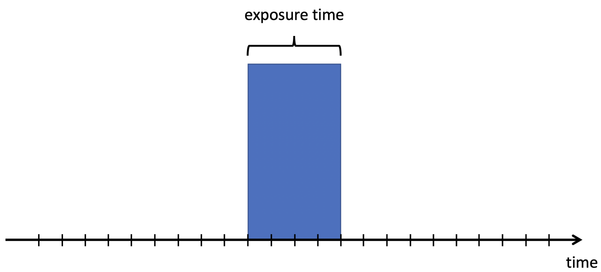

Fig. 3. Temporal rectangular kernel with sensor exposure time as its support.

reconstruct fast progressing phenomena that were corrupted spatially by the microwave aperture synthesis system's point spread function (PSF) and temporally by averaging.

II. The Geostationary Synthetic Thinned Aperture Radiometer (GeoSTAR)

Observations of atmospheric wind, storm processes, and boundary layer processes are essential for assessing weather and climate. Critical regions within dynamic weather systems are commonly either (1) obscured by clouds and rain, where microwave sounders have a large advantage over other sensors, or (2) rapidly evolving, where geostationary sensors have a large advantage over low-orbiting satellites. GeoSTAR is a geostationary microwave spectrometer aperture synthesis sounder concept that has been developed at the Jet Propulsion Laboratory (JPL) that can provide such observations. It measures 3-D fields of temperature, water vapor, clouds, precipitation and wind in a large area below the host satellite. Its spatial kernel is a 2-D sinc-like function with positive and negative sidelobes (cf. Fig. 2), which blurs the resulting images and creates artifacts. Also, temporal blurring (cf. Fig. 3) occurs when the scene evolves faster than the sensor refresh cycle, such as with intense convective precipitation [21]. While the spatial and temporal resolutions that can be achieved with GeoSTAR are on the order of 25 km and 15 minutes, more measurement objectives can be met with 10-15 km and 5-10 minutes. GeoSTAR produces spatio-temporal oversampling that lends itself to digital resolution enhancement techniques. We have previously developed and published methodologies [14]–[16] to enhance spatial resolution and temporal resolution separately, but not both at the same time. That is the focus

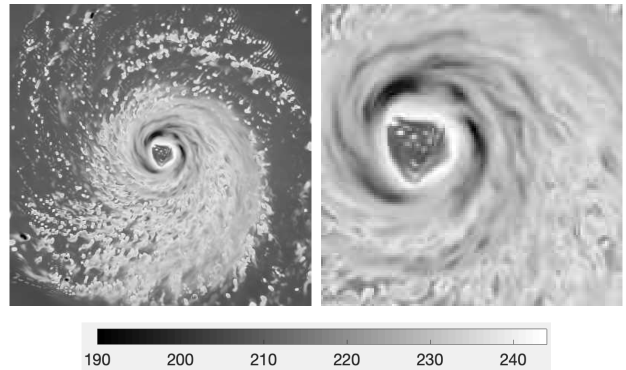

(a) 50.3 GHz

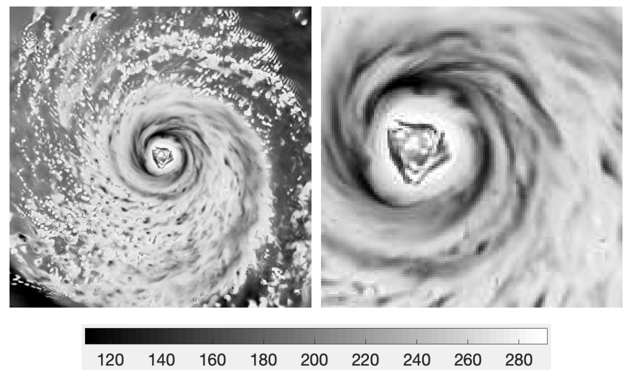

(b) 150 GHz

Fig. 4. One of 36 original 402x402 pixel frames of (a) 50.3 GHz and (b) 150 GHz microwave image sequences of the simulated hurricane Rita and their zoomed in regions are shown. The size of the pixel is 1.3 km.

of this paper. With such a methodology, the value of the GeoSTAR observations would be greatly enhanced.

III. Spatio-Temporal Resolution Reconstruction

An image sequence could be captured by a sensor that convolves an observed scene with a spatio-temporal point spread function whose two-dimensional spatial component is the microwave instrument's point spread function and whose one-dimensional temporal component is the rectangular kernel with sensor exposure time as its support. The spatial blurring and distortion are induced by microwave aperture synthesis system. The temporal blurring occurs when multiple frames are averaged. To visualize space-time blurring, we can consider the spatio-temporal volume (cf. Fig. 1) being smoothed in spatial domain using microwave PSF and in temporal direction using averaging.

We consider a multi-frame sequence of P images. Each image has $M \times N$ pixels. Such a sequence is denoted as $g_0 \in \mathbb{R}^{M \times N \times P}$ (cf. Fig. 1). The spatio-temporal convolution and additive noise model for a corrupted sequence f is given as

$$f = K * g_0 + \kappa, \tag{1}$$

where K is a spatio-temporal convolution kernel and κ is additive noise.

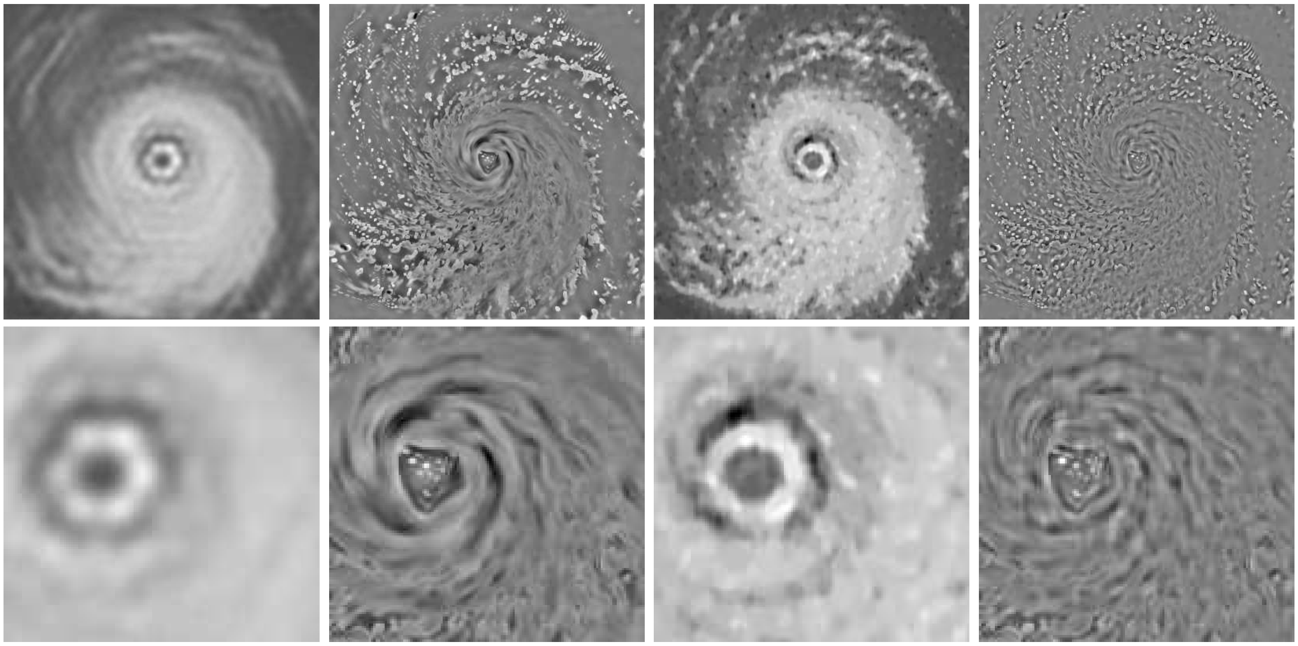

(a) Blurry and noisy 50.3GHz frame

(b) Initial Error. SNR = 4.49, RMSE = 5.97K

(c) Reconstructed frame

(d) Final Error. SNR = 6.49, RMSE = 4.74K

Fig. 5. Spatio-temporal resolution enhancement of an image sequence in Figure 4(a). (a) Original sequence, a single frame of which is shown in Figure 4(a), is convolved with spatio-temporal convolution kernel whose two-dimensional spatial component is the GeoSTAR kernel from Figure 2 and whose one-dimensional temporal component is the temporal rectangular function from Figure 3. The sequence is subject to Gaussian noise of variance $\sigma^2 = 2K^2$. (b) Corresponding error in (a). (c) Spatio-temporal enhancement reconstruction result. (d) Corresponding error in (c).

In oder to reconstruct the sequence, we use the TV norm

$$||g||_{\text{TV}} = \int |\nabla g|.$$

TV minimization preserves the features in an image. The TV-L_2 deconvolution minimization problem is given as

$$\min_{g} \quad ||g||_{\text{TV}} + \frac{\mu}{2}||K * g - f||_2^2, \tag{2}$$

where $\mu > 0$ is a weighting parameter, and g is a space-time reconstruction. The problem in (2) is solved using the Split Bregman method.

IV. Results

In our experiments, we used a simulated microwave 50.3 and 150 GHz channel image sequences of a hurricane Rita from 2005 (cf. Fig. 4). The Advanced Microwave Sounding Unit - A (AMSU-A) temperature sounder and AMSU-B water vapor sounder have some of the same frequencies of GeoSTAR near 55 GHz and 180 GHz, respectively. The simulations were generated at the Jet Propulsion Laboratory (JPL) using the Weather Research and Forecast (WRF) model [22]. Each sequence contains 36 images which are 10 minutes apart. Each image is 402 $\times$ 402 pixels. The size of the pixel is 1.3 km. The spatio-temporal convolution kernel, whose two-dimensional spatial component is the GeoSTAR kernel and whose one-dimensional temporal component is the temporal rectangular function, was used to blur the image sequences. The GeoSTAR point spread function is 101 $\times$ 101, with 27.6 km of full width at half maximum, and is displayed in Figure 2. The temporal rectangular kernel is 5 frames wide and is shown in Figure 3. We note that the GeoSTAR kernel is more difficult to deconvolve than Gaussian kernel. Also, a wide temporal kernel amounts to a considerable averaging. Such degradations result in corrupted image sequences (cf. Fig. 5(a) and 6(a)) that do not resemble original image sequences in Figure 4.

Figure 5(a) displays the 50.3 GHz sequence of images of Figure 4(a) subject to the spatio-temporal blur and Gaussian noise of variance $\sigma^2 = 2K^2$. Figure 5(b) shows the corresponding error of the sequence in Figure 5(a) relative to the original sequence of images in Figure 4(a) as well as gives signal-to-noise ratio (SNR) and root mean square (RMS) error values. The spatio-temporal reconstruction result is displayed in Figure 5(c), and the corresponding error is displayed in Figure 5(d). In Figures 5(a) and 5(b) we notice the artificial ringing due to GeoSTAR PSF. Figure 5(c) displays an image sequence that resembles the sequence in Figure 4(a) while improving the accuracy when compared to the observed sequence.

Figures 4(b) and 6 show similar results but for the 150 GHz image sequence.

References

[1] D. Kundur and D. Hatzinakos, "Blind image deconvolution," *IEEE Signal Processing Magazine*, vol. 13, no. 3, pp. 43–64, 1996.

[2] D. G. Long and D. L. Daum, "Spatial resolution enhancement of SSM/I data," *IEEE Transactions on Geoscience and Remote Sensing*, vol. 36, no. 2, pp. 407–417, 1998.

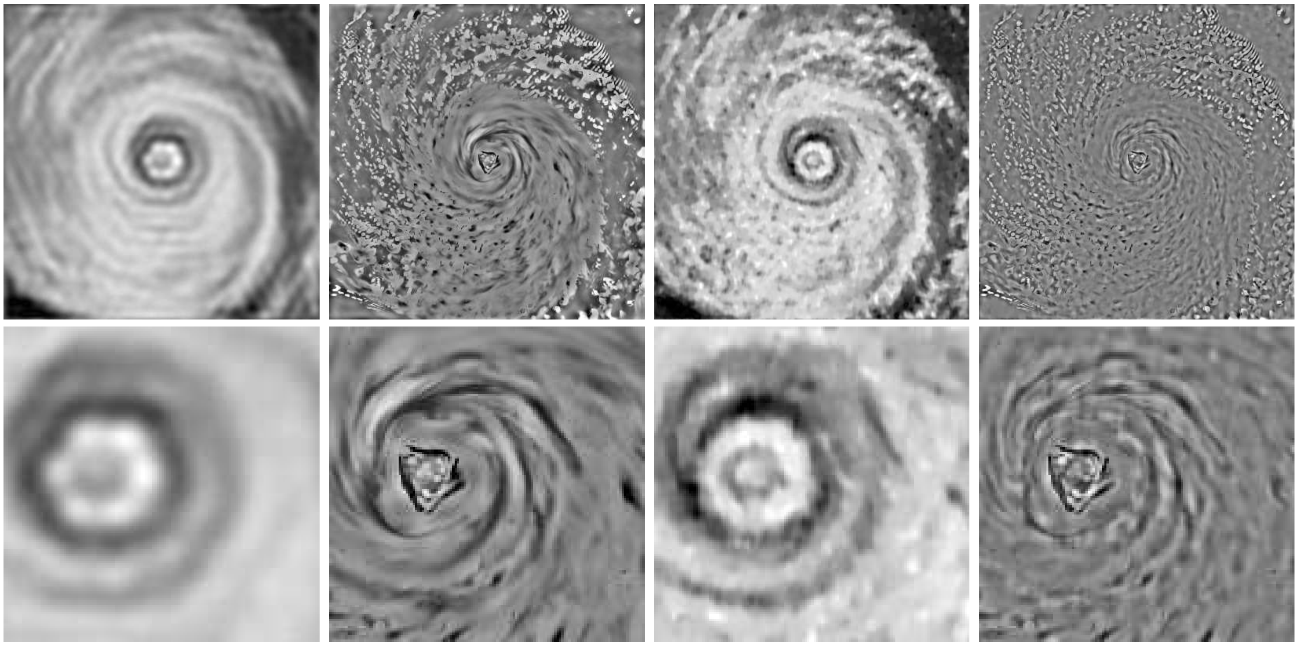

(a) Blurry and noisy 150GHz frame

(b) Initial Error. SNR = 4.00, RMSE = 25.59K

(c) Reconstructed frame

(d) Final Error. SNR = 6.21, RMSE = 19.84K

Fig. 6. Spatio-temporal resolution enhancement of an image sequence in Figure 4(b). (a) Original sequence, a single frame of which is shown in Figure 4(b), is convolved with spatio-temporal convolution kernel whose two-dimensional spatial component is the GeoSTAR kernel from Figure 2 and whose one-dimensional temporal component is the temporal rectangular function from Figure 3. The sequence is subject to Gaussian noise of variance $\sigma^2 = 2K^2$. (b) Corresponding error in (a). (c) Spatio-temporal enhancement reconstruction result. (d) Corresponding error in (c).

[3] N. R. Shah and A. Zakhor, "Resolution enhancement of color video sequences," *IEEE Transactions on Image Processing*, vol. 8, no. 6, pp. 879–885, 1999.

[4] J.-L. Starck, M. K. Nguyen, and F. Murtagh, "Wavelets and curvelets for image deconvolution: a combined approach," *Signal Processing*, vol. 83, no. 10, pp. 2279 – 2283, 2003.

[5] A. C. Likas and N. P. Galatsanos, "A variational approach for bayesian blind image deconvolution," *IEEE Transactions on Signal Processing*, vol. 52, no. 8, pp. 2222–2233, 2004.

[6] M. Migliaccio and A. Gambardella, "Microwave radiometer spatial resolution enhancement," *IEEE Transactions on Geoscience and Remote Sensing*, vol. 43, no. 5, pp. 1159–1169, 2005.

[7] J. M. Bioucas-Dias, M. A. T. Figueiredo, and J. P. Oliveira, "Total variation-based image deconvolution: a majorization-minimization approach," in *2006 IEEE International Conference on Acoustics Speech and Signal Processing Proceedings*, vol. 2, 2006, pp. II–II.

[8] D. Krishnan and R. Fergus, "Fast image deconvolution using hyper-laplacian priors," in *Advances in Neural Information Processing Systems*, Y. Bengio, D. Schuurmans, J. Lafferty, C. Williams, and A. Culotta, Eds., vol. 22. Curran Associates, Inc., 2009, pp. 1033–1041.

[9] M. Piles, A. Camps, M. Vall-llossera, and M. Talone, "Spatial-resolution enhancement of SMOS data: A deconvolution-based approach," *IEEE Transactions on Geoscience and Remote Sensing*, vol. 47, no. 7, pp. 2182–2192, 2009.

[10] S. Posse, E. Ackley, R. Mutihac, J. Rick, M. Shane, C. Murray-Krezan, M. Zaitsev, and O. Speck, "Enhancement of temporal resolution and BOLD sensitivity in real-time fMRI using multi-slab echo-volumar imaging," *NeuroImage*, vol. 61, no. 1, pp. 115 – 130, 2012.

[11] D. Ryu, Z. Wang, K. He, G. Zheng, R. Horstmeyer, and O. Cossairt, "Subsampled phase retrieval for temporal resolution enhancement in lensless on-chip holographic video," *Biomed. Opt. Express*, vol. 8, no. 3, pp. 1981–1995, Mar 2017.

[12] A. Eichenseer, M. Batz, and A. Kaup, "Motion estimation for fisheye video with an application to temporal resolution enhancement," *IEEE Transactions on Circuits and Systems for Video Technology*, vol. 29, no. 8, pp. 2376–2390, 2019.

[13] K. Makki, B. Borotikar, M. Garetier, S. Brochard, D. B. Salem, and F. Rousseau, "Temporal resolution enhancement of dynamic MRI sequences within a motion-based framework," in *2019 41st Annual International Conference of the IEEE Engineering in Medicine and Biology Society (EMBC)*, 2019, pp. 4004–4007.

[14] I. Yanovsky, B. Lambrigtsen, A. Tanner, and L. Vese, "Efficient deconvolution and super-resolution methods in microwave imagery," *IEEE Journal of Selected Topics in Applied Earth Observations and Remote Sensing*, vol. 8, no. 9, pp. 4273–4283, 2015.

[15] J. Qin, I. Yanovsky, and W. Yin, "Efficient simultaneous image deconvolution and upsampling algorithm for low resolution microwave sounder data," *Journal of Applied Remote Sensing*, vol. 9, no. 1, pp. 095 035/1–15, 2015.

[16] I. Yanovsky and B. Lambrigtsen, "Temporal super-resolution of microwave remote sensing images," in *2018 IEEE 15th Specialist Meeting on Microwave Radiometry and Remote Sensing of the Environment (MicroRad)*, 2018, pp. 110–115.

[17] L. Rudin, S. Osher, and E. Fatemi, "Nonlinear total variation based noise removal algorithms," *Physica D*, vol. 60, pp. 259–268, 1992.

[18] T. Goldstein and S. Osher, "The split bregman method for L1-regularized problems," *SIAM Journal on Imaging Sciences*, vol. 2, no. 2, pp. 323–343, 2009.

[19] E. Shechtman, Y. Caspi, and M. Irani, "Space-time super-resolution," *IEEE Transactions on Pattern Analysis and Machine Intelligence*, vol. 27, no. 4, pp. 531–545, 2005.

[20] S. H. Chan, R. Khoshabeh, K. B. Gibson, P. E. Gill, and T. Q. Nguyen, "An augmented lagrangian method for total variation video restoration," *IEEE Transactions on Image Processing*, vol. 20, no. 11, pp. 3097–3111, 2011.

[21] B. Lambrigtsen, T. Gaier, P. Kangaslahti, B. Lim, A. Tanner, and C. Ruf, "Enabling the NASA decadal-survey "PATH" mission," in *2016 IEEE International Geoscience and Remote Sensing Symposium (IGARSS)*, 2016, pp. 3949–3951.

[22] J. Michalakes, J. Dudhia, D. Gill, J. Klemp, and W. Skamarock, *Design of a next-generation regional weather research and forecast model: Towards Teracomputing*. River Edge, New Jersey: World Scientific, 1998.